Accepted Manuscript

Evaluation of air oxidized PAPC: A multi laboratory study by LC-MS/MS

Zhixu Ni, Bebiana C. Sousa, Simone Colombo, Catarina B. Afonso, Tania Melo, Andrew R. Pitt, Corinne M. Spickett, Pedro Domingues, M. Rosário Domingues, Maria Fedorova, Angela Criscuolo

PII: S0891-5849(19)30347-8

DOI: https://doi.org/10.1016/j.freeradbiomed.2019.06.013

Reference: FRB 14312

To appear in: *Free Radical Biology and Medicine*

Received Date: 28 February 2019

Revised Date: 29 May 2019

Accepted Date: 10 June 2019

Please cite this article as: Z. Ni, B.C. Sousa, S. Colombo, C.B. Afonso, T. Melo, A.R. Pitt, C.M. Spickett, P. Domingues, M.Rosá. Domingues, M. Fedorova, A. Criscuolo, Evaluation of air oxidized PAPC: A multi laboratory study by LC-MS/MS, *Free Radical Biology and Medicine* (2019), doi: https://doi.org/10.1016/j.freeradbiomed.2019.06.013.

Evaluation of air oxidized PAPC: a multi laboratory study by LC-MS/MS.

Zhixu Ni[1,2#], Bebiana C. Sousa[3#], Simone Colombo[4], Catarina B. Afonso[3], Tania Melo[4,5], Andrew R. Pitt[3], Corinne M. Spickett[3], Pedro Domingues[4], M. Rosário Domingues[4], Maria Fedorova[1,2], Angela Criscuolo[1,2,6] *

[1]Institute of Bioanalytical Chemistry, Faculty of Chemistry and Mineralogy, University of Leipzig, Germany; [2]Center for Biotechnology and Biomedicine, University of Leipzig; [3]School of Life & Health Sciences, Aston University, Aston Triangle, Birmingham B4 7ET, UK; [4]Mass Spectrometry Centre, Department of Chemistry & QOPNA, University of Aveiro, Campus Universitário de Santiago, 3810-193 Aveiro, Portugal; [5]Department of Chemistry & CESAM&ECOMARE, University of Aveiro, Campus Universitário de Santiago, 3810-193 Aveiro, Portugal; [6]Thermo Fisher Scientific (Bremen) GmbH, Hanna-Kunath-Str. 11, 28199 Bremen, Germany.

[#] These authors made an equal contribution.

Corresponding author:

* Angela Criscuolo, Thermo Fisher Scientific (Bremen) GmbH, Hanna-Kunath-Str. 11, 28199 Bremen, Germany. E-mail: angela.criscuolo@thermofisher.com

Keywords

Oxidized phospholipids, PAPC, reverse phase chromatography, tandem mass spectrometry, multi-laboratory study

Abbreviation

CID: collision-induced dissociation; CV: coefficient of variation; DAMP: damage associated molecular pattern; DMPC: 1,2-dimyristoyl-*sn*-glycero-3-phosphocholine; HCD: high-energy collisional dissociation; HOOAPC: 1-palmitoyl-2-(5-hydroxy-8-oxo-octenoyl)-*sn*-glycero-3-phosphorylcholine; LC-MS/MS: Liquid chromatography coupled on-line to tandem mass spectrometry; LPC: lysophosphatidylcholine; LPP: lipid peroxidation product; oxLDL: oxidized LDL; oxPL: oxidized phospholipid; PAPC: 1-palmitoyl-2-arachidonoyl-*sn*-glycero-

3-phosphocholine; PC: phosphatidylcholine; PEIPC: 1-palmitoyl-2-epoxyisoprostaneE2-*sn*-glycero-3-phosphocholine; PGPC: 1-palmitoyl-2-glutaryl-*sn*-glycero-3-phosphocholine; POVPC: 1-palmitoyl-2-(5-oxovaleroyl)-*sn*-glycero-3-phosphorylcholine; PL: phospholipid; TS: truncation score; XIC: Extracted ion chromatograms.

Abstract

Oxidized LDL (oxLDL) has been shown to play a crucial role in the onset and development of cardiovascular disorders. The study of oxLDL, as an initiator of inflammatory cascades, led to the discovery of a variety of oxidized phospholipids (oxPLs) responsible for pro-inflammatory actions. Oxidized 1-palmitoyl-2-arachidonoyl-*sn*-glycero-3-phosphocholine (PAPC) is frequently used by the scientific community as a representative oxPL mixture to study the biological effects of oxidized lipids, due to the high abundance of PAPC in human tissues and the biological activities of oxidized arachidonic acids derivatives. Most studies focusing on oxPAPC effects rely on in-house prepared mixtures of oxidized species obtained by exposing PAPC to air oxidation. Here, we described a multi-laboratory evaluation of the compounds in oxPAPC by LC-MS/MS, focusing on the identification and relative quantification of the lipid peroxidation products (LPPs) formed. PAPC was air-oxidized in four laboratories using the same protocol for 0, 48, and 72 hours. It was possible to identify 55 different LPPs with unique elemental composition and characterize different structural isomeric species within these. The study showed good intra-sample reproducibility and similar qualitative patterns of oxidation, as the most abundant LPPs were essentially the same between the four laboratories. However, there were substantial differences in the extent of oxidation, i.e. the amount of LPPs relative to unmodified PAPC, at specific time points. This shows the importance of characterizing air-oxidized PAPC preparations before using them for testing biological effects of oxidized lipids, and may explain some variability of effects reported in the literature.

Graphical Abstract

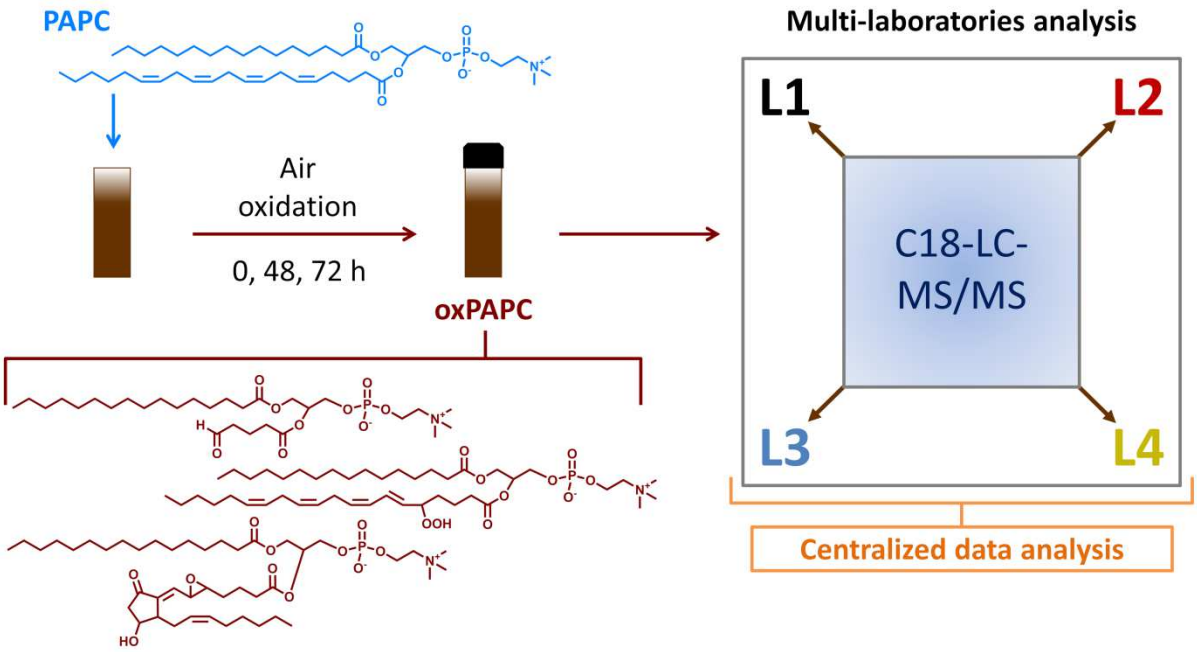

1. Introduction

The role of oxidized LDL as an initiator of inflammatory cascades that contribute to the pathogenesis of cardiovascular disorders including atherosclerosis, led to the discovery of a variety of oxidized phospholipids (oxPLs) important for the fine tuning of innate and adaptive immune responses [1–3]. OxPLs formed via enzymatic or free-radical driven reactions are closely associated with systemic redox imbalance and low-grade chronic inflammation, and thus have been intensively studied from structural, chemical, biophysical, and biological perspectives over the last decades[4–8]. Within the generic classification of oxPL, the oxidation products of 1-palmitoyl-2-arachidonoyl-*sn*-glycero-3-phosphocholine (PAPC), which have been identified as some of the bioactive components in minimally modified LDL, are the oxPLs most often used to study the biological effects of oxidized lipids [9]. Furthermore, PAPC is among the most abundant PLs in human tissues [10]. Arachidonic acid, present in the *sn*-2 position of PAPC, can form a very diverse range of oxidation products, many of which have already been shown to be bioactive in their free fatty acid forms. Indeed, numerous studies have demonstrated the pro- and anti-inflammatory properties of, for example, eicosanoids, which are generated from arachidonic acid via action of dedicated enzymes or free radical driven lipid peroxidation [11–13]. However, the action of PC-esterified eicosanoids has been relatively less well studied.

A variety of bioactivities have been attributed to oxidized PAPC (oxPAPC). It has been identified as a major pro-atherogenic factor and pro-inflammatory mediator [14,15], but in contrast anti-inflammatory properties of oxPAPC have also been demonstrated [13,16]. OxPAPC has been shown to induce both the disruption as well as enhancement of the endothelial barrier [17,18], and recently a pro-algesic effect of oxPAPC, via stimulation of transient receptor potential channels TRPA1 and TRPV1, was demonstrated [19,20]. OxPAPC was also shown to act as a damage associated molecular pattern (DAMP), activating classical and non-classical pattern recognition receptors. Thus, oxPAPC released from injured tissues was shown to be recognized by murine caspase-11 and CD14 leading to inflammasome activation and release of pro-inflammatory cytokines, and this pathway demonstrated differential regulation in macrophages and dendritic cells [21–23]. The variety of biological effects of oxPAPC are well established and their conflicting properties have been discussed recently [24–26].

One of the main obstacles in elucidating the effects oxPLs on biological systems is the almost complete lack of commercially available and chemically characterized standards for each individual oxPL product. Thus, to study their biological properties, a mixture of

products, usually referred to as "oxPAPC" is often used. The majority of the studies on oxPAPC effects rely on commercial or in-house preparations, usually obtained by exposing a dried film of PAPC to air oxidation for up to 72 h. Experimental details such as room temperature, light exposure, thickness of the phospholipid film and oxPAPC quality control are usually not provided. Given the variety of biological functions attributed to oxPAPC in different cellular and *in vivo* models, which may be dependent on variations in sample preparation affecting the precise composition of the oxPAPC, we performed a multi-laboratory study with the aim of evaluating the reproducibility of PAPC oxidation upon air exposure for 48 and 72 h. Liquid chromatography coupled on-line to tandem mass spectrometry (LC-MS/MS) was used to identify lipid peroxidation products (LPPs) formed upon PAPC oxidation, and the relative quantities of LPPs formed were compared between samples generated independently in four different international laboratories.

2. Materials and Methods

2.1. Materials

1-palmitoyl-2-arachidonoyl-sn-glycero-3-phosphocholine and 1,2-dimyristoyl-sn-glycero-3-phosphocholine were purchased from Avanti Polar Lipids (Avanti Polar Lipids, Inc., Alabama, USA). In laboratory 1 (L1) acetonitrile, isopropanol, water, methanol, ammonium formate (Optima LC-MS grade), chloroform and formic acid (LC-MS grade) were obtained from Fisher Scientific (Loughborough, UK). In laboratory 2 (L2) HPLC-MS grade chloroform, methanol, acetonitrile and isopropanol were purchased from Fisher Scientific (Leicestershire, UK). Formic acid was from Honeywell Fluka (Neu Wulmstorf, Germany). Ammonium formate was obtained from Sigma-Aldrich (Sigma-Aldrich, Munich, Germany). The water was of Milli-Q purity (Synergy1, Millipore Corporation, Billerica, MA). In laboratory 3 (L3) acetonitrile, isopropanol, water, methanol, ammonium formate (Optima^{TM} LC/MS grade) and chloroform (LC/MS grade) were obtained from Fisher Scientific (Schwerte, Germany). Formic acid (LC-MS grade) was purchased from Sigma-Aldrich (Sigma-Aldrich, Munich, Germany). In laboratory 4 (L4) acetonitrile, isopropanol, methanol, and formic acid (all ULC-MS grade) were from Biosolve (Valkenswaard, Netherlands). Ammonium formate and chloroform were from Sigma-Aldrich GmbH (Taufkirchen, Germany).

2.2. OxPAPC preparation.

OxPAPC was prepared either in one laboratory (L3) or independently in four participating laboratories following the protocol describe below. A mixture of 1-palmitoyl-2-

linoleoyl-*sn*-glycero-3-phosphocholine (PAPC; 50 µg) and 1-2-dimiristoyl-*sn*-glycero-3-phosphocholine (DMPC; 2.2 µg; a fully saturated PC used as internal standard for relative quantification) in chloroform was dried under a stream of N_2 in a 2 mL amber flat bottom vial to form a thin film at the vial bottom (three independent replicates). The lipid film was exposed to air at room temperature (L1 – 22-25°C, L2 – 16°C, L3 – 28°C, L4 – 25°C) for 0, 48 and 72 hours. After incubation the vial was filled with N_2, tightly sealed and stored at -80°C. Samples from L3 were sent to the other laboratories on freezer blocks at -20°C .

2.3. LC-MS/MS analysis.

The experimental replicates (n=3) of sample prepared in L3 (0 and 72 h of oxidation; analysed by L1, L3, and L4), as well as samples generated independently in each of the four participating laboratories and analysed there, were used to assess inter-laboratory variability. In L4, experimental replicate 1 was analysed in triplicate on three consecutive days, to assess intra- and inter-day analytical variability. Comparable chromatographic conditions and the best available tandem MS instrument were used in the 4 laboratories. Details on LC-MS/MS are provided in **Table 1** and Supplementary Methods section. Briefly, UHPLC separations were performed on C18 reverse phase columns using binary solvent systems containing water, acetonitrile, methanol and isopropanol, with ammonium formate (5 mmol/L) and formic acid (0.1%) as additives [27]. MS analyses were performed using data-dependent acquisition (DDA) in positive and negative ion modes (**Table 1** and Supplementary Methods).

2.4. Automated identification of lipid peroxidation products (LPPs).

LPPtiger software source code version was used for lipid identification ([28]; https://bitbucket.org/SysMedOs/lpptiger). PAPC was oxidized *in silico* using theoretical oxidation level 2. The list of modifications included hydroperoxy, hydroxy, epoxy, and keto groups with the maximum number equal to the number of bis-allylic and allylic sites in the structure. The oxidative cleavage products with aldehyde and carboxylic acid on the terminal carbon were included. LPPtiger predicted 345 unique oxidized fatty acyl chains corresponding to 692 discrete oxPAPC species including lyso species. All raw spectra were converted into mzML format using ProteoWizard MSconvert (Version 3.0.9134 64bit) and the following parameters were used for all files: *m/z* range 400 to 1000, isotope score filter 80, and overall score filter 40. For L1 files 50 ppm on MS level and 200 ppm on MS2 level were used as mass tolerance thresholds. For L2, L3, and L4 mass tolerance of 10 ppm on MS and MS2 levels was applied. Analysis was performed using the integrated batch mode of LPPtiger on a workstation equipped with 2 CPUs (32 cores) and 128 GB of RAM in L4.

2.5. Relative LPPs quantification.

15 LPPs detected in all four laboratories and previously reported in the literature as a component of oxPAPC [9,11,13,14,16–18,23,29,30] were chosen for the relative quantification (**Table 2**). Peak area for each lipid was integrated and normalized relative to the DMPC lipid used as non-oxidizable internal standard. Average percent values for each LPP relative to PAPC were calculated using normalized peak areas.

2.6. Statistical analysis.

Coefficient of variation (CV%) was calculated using the following equation CV% = DevSTD/AverageRelativeArea*100 for each LPPs using normalized peak areas. Principal component analysis was performed using normalized peak area of 15 LPPs from L3 prepared samples analyzed by three laboratories (L1, L3 and L4) using EZinfo (version 1.0, MKS Instruments, Crewe, UK). ANOVA (Single Factor) analysis was performed by Analysis ToolPak Excel Add-In for each LPPs using normalized peak areas.

2.7. Nomenclature.

Lipid nomenclature is based on the LIPID MAPS consortium recommendations [31]. For instance, the shorthand notation PC 36:4 represents a phosphatidylcholine lipid containing 36 carbons and four double bonds. When the fatty acid identities and *sn*-position are known, as in our case, the slash separator is used (e.g., PC 16:0/20:4). Since no unified nomenclature is available for oxidized lipids, the short hand notations provided by LPPtiger tool were used [28]. Short chain oxidized lipids were indicated by the corresponding terminal enclosed in angular brackets (e.g. “<” and “>”), with the truncation site indicated by the carbon atom number (e.g., <COOH@C9> and <CHO@C12). For long chain products our recommendation is to indicate the number of oxygen addition after the fully identified parent lipid (e.g. PC 16:0/20:4 + 1O) when the type of addition is not known, or in parenthesis for known functional groups (e.g. PC 16:0/20:4[1xOH@C11]).

197 **Table 1.** Summary of LC-MS/MS methods used for the analysis of oxPAPC in four different
198 laboratories.

	L1	L2	L3	L4
Chromatography				
Column	Accucore™ C18	ACE C18	Accucore™ C18	Accucore™ C18
Column phase	Solid core, C18	Solid core, C18	Solid core, C18	Solid core, C18
Dimensions	150 x 2.1 mm	150 x 0.5 mm	150 x 2.1 mm	150 x 2.1 mm
Particle size	2.6 µm	5 µm	2.6 µm	2.6 µm
Pore size	150 Å	100 Å	150 Å	150 Å
Gradient	isopropanol: acetonitrile: water	isopropanol: methanol: acetonitrile: water	isopropanol: acetonitrile: water	isopropanol: acetonitrile: water
Temperature	50 °C	40 °C	50 °C	50 °C
Tandem MS				
Instrument	5600 TripleTOF	Q Exactive™	Orbitrap Fusion™ Lumos™ Tribrid™	Q Exactive™ Plus
MS1	200-1500 *m/z*	400–1200 *m/z*	450–1200 *m/z*	380–1200 *m/z*
Resolution	High sensitivity	70,000	120,000	140,000
DDA top #	5	5	15	10
Fragmentation	CID	HCD	HCD	HCD
CE	35V, 10V CES	NCE 20, 23, 25	NCE 20 +/- 10	NCE 18 +/- 6
Resolution MS2	High sensitivity	17,500	15,000	17,500

199

3. Results and Discussion

3.1. Identification of LPP species in air oxidized PAPC.

To evaluate the extent of PAPC oxidation and identify the LPPs formed, oxPAPC samples prepared in four different laboratories (L1-L4) were analysed by LC-MS/MS using reverse phase separation on C18 columns and data-dependent acquisition on four different MS instruments (**Table 1**). OxPAPC mixtures were analysed in both positive and negative ion modes. Positive ion mode data were used for relative quantification, given the higher ionization efficiency of PC lipids as protonated quasi-molecular ions, whereas the negative ion mode data were used for identification of LPPs based on tandem mass spectra of the formate adduct or deprotonated ions, as the negative ion fragmentation data contains informative fragment anions of the modified acyl chains.

Fig. 1 shows representative positive ion mode base peak chromatograms for three different time points of PAPC oxidation obtained from the four laboratories. Representative negative ion mode base peak chromatograms are shown in **Supplementary Fig. S1**. DMPC, which contains two fully saturated C14:0 acyl chains, was spiked into all preparation at equal quantities (PAPC:DMPC, 20:1 molar ratio) and was used as an internal standard for relative quantification. The general pattern of oxidation was very similar between all laboratories. At the 0 h time point two main signals, corresponding to DMPC (*m/z* 678. 51^{+}) and native PAPC (*m/z* 782. 57^{+}), are clearly visible, with almost a complete absence of LPPs. After 48 h of air exposure, a large number of signals for analytes with shorter retention times than PAPC can be observed, indicating the presence of species with higher polarities than native PAPC. After 72 h, most of the signals eluted towards the beginning of chromatographic gradients, generally in the first third, corresponding to chain-shortened oxidation products, accompanied by a corresponding decrease of the signals eluting in the middle third of the gradient, corresponding to long-chain oxidised products, as well a decrease the native PAPC signal which appears towards the end of the gradient.

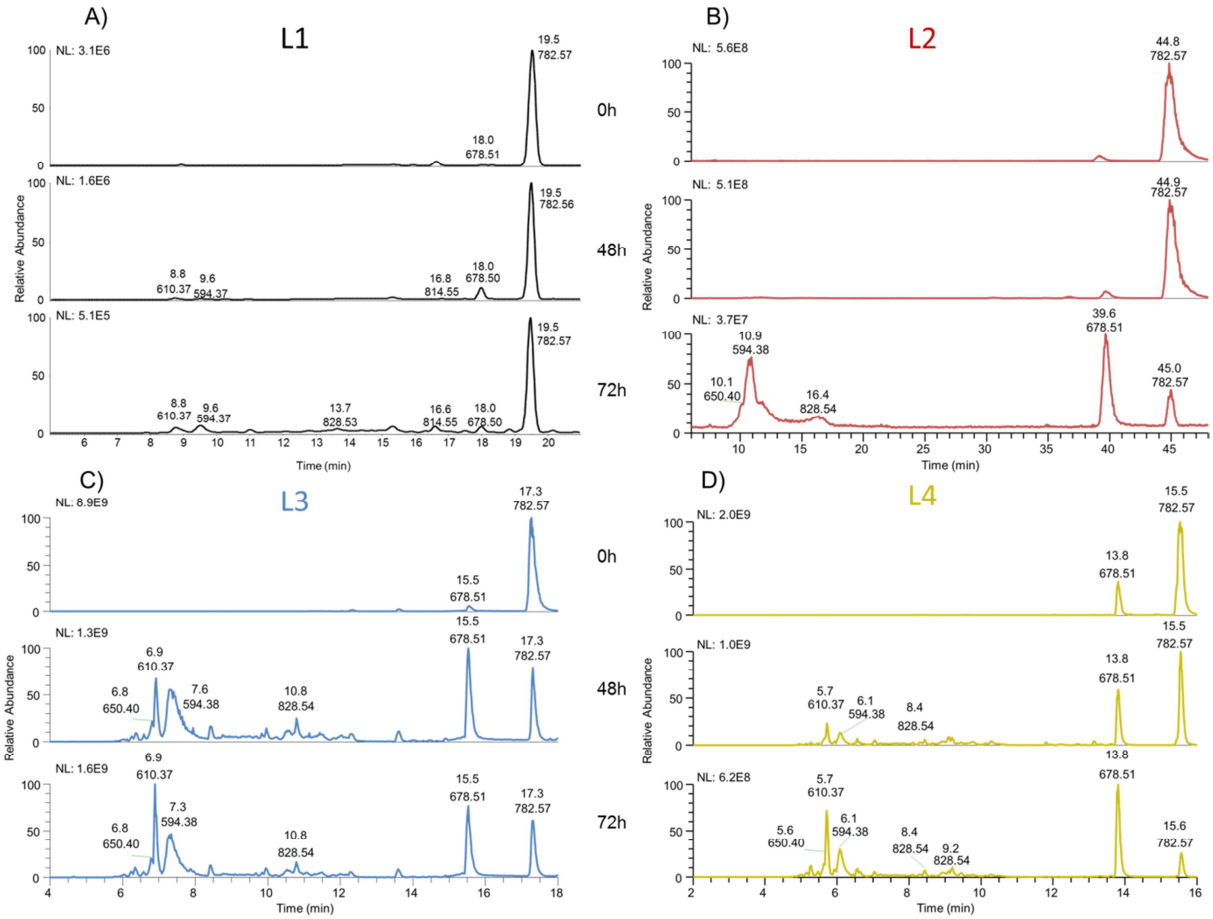

Fig. 1. Positive ion mode base peak chromatograms of PAPC lipid oxidized by air exposure for 0, 48 and 72 h and analysed using reverse phase chromatography coupled on-line to tandem mass spectrometry detection in L1 (A), L2 (B), L3 (C) and L4 (D).

LPPtiger, a new software for the identification of oxidized phospholipids from data-dependent LC-MS/MS datasets, was used for the automated identification of LPPs in the oxPAPC preparations [28]. LPPtiger performs identification based on the fragment ions observed in CID or HCD experiments in the negative ion mode. The presence of specific anions corresponding to native and oxidized acyl chains in PLs allows identification of the oxidation type, whereas fragment ions and specific neutral losses provides identification of PL class. Identification of positional isomers of oxPL is not supported by the current version of the software, but the MS/MS based identification of oxidized fatty acyl chains together with isotopic scores correction provide a solid basis for the identification of molecular species.

Overall 55 different LPPs with unique elemental compositions were identified, providing 143 potential LPPs after considering functional group isomers (**Supplementary**

Table S1). The 55 identified LPPs covered a number of different types of oxidative products, including the lysophosphatidylcholines (LPC) LPC(16:0) and LPC(20:4), as well as 40 short chain and 15 long chain LPPs. 24 LPPs were identified by all three laboratories that performed DDA analysis (L2 used an inclusion list function and thus was not considered for this comparison), and 45 LPPs were identified by two laboratories. Overall, all of the main LPPs generally regarded as being present in oxPAPC mixtures were successfully identified by LPPtiger at the MS/MS level, including the truncated species 1-palmitoyl-2-(5-oxovaleroyl)-*sn*-glycero-3-phosphorylcholine (POVPC; *m/z* 594.38^{+}) and 1-palmitoyl-2-glutaryl-*sn*-glycero-3-phosphocholine (PGPC; *m/z* 610.37^{+}), long chain products with hydroperoxy, hydroxy, and keto groups, and 1-palmitoyl-2-epoxyisoprostaneE2-*sn*-glycero-3-phosphocholine (PEIPC; *m/z* 828.54^{+}).

The different numbers of LPPs identified by LPPtiger from the MS/MS data from the four laboratories most probably relates to the differences in MS methods and instruments used in the study. Thus, the highest number of LPPs was identified by L3 utilizing a Tribid Orbitrap Fusion Lumos, which is capable of acquiring a high number of tandem mass spectra (15 MS/MS) per one survey scan, followed by L4 and L1 in which top 10 and top 5 DDA methods were applied using a Q Exactive™ Plus and a TripleToF 5600 respectively. L2 performed targeted acquisition using inclusion lists for 63 LPPs, of which 12 were successfully identified.

3.2. LC-MS/MS based identification of isomeric LPPs.

Reverse phase chromatographic separation allowed the resolution of multiple isomeric LPP species. The C18 phase proved to be a good stationary phase for the separation of the relatively polar analytes formed by the oxidation of PLs, which are characterized by a mid-range polarity compared to the other lipid classes. Reverse phase separation strongly depends on the hydrophobicity of the analyte, usually described by the partition coefficients logP and logD [32], along with to a lesser extent some other physico-chemical properties, such as dipole-dipole interactions, proton acceptor/donor interactions and analyte polarizability. In comparison with native PAPC, which has a logP 8.4, introduction of a single hydroxy group results a shift of the logP to 7.2, whereas presence of three hydroxy groups or the isoprostane ring structures (e.g. PGF2α) further shifts the logP values further to 5.1 and 4.5, respectively. The use of a C18 stationary phase with an isopropanol-acetonitrile-water elution gradient ensures optimal binding of these mid-polarity lipid analytes while still providing efficient separation of lipid species. The combination of LC separation with tandem mass

spectrometry allows the acquisition of separate tandem mass spectra for the separated isomeric LPPs, and CID or HCD fragment spectra acquired in the negative ion mode provides the information necessary to identify the type and often the position of the modification.

Fig. 2 illustrates three examples of LC-MS/MS based identification of short chain oxPAPC species.

Extracted ion chromatograms (XICs) for POVPC (**Fig. 2**) in negative ([M+HCOOH-H^+], *m/z* 638.37) and positive ([M+H^+], *m/z* 594.38) ion modes both had two chromatographic peaks with a retention times of 5.6 and 6.1 min. Although the POVPC signal was already present at the 0 h oxidation time point, the intensity of this LPP increased by more than two orders of magnitude over the oxidation time course (e.g. from 5e4 counts at 0h to 8e6 counts at 72 h for the example shown in **Fig. 2** of the analysis performed by L3). The positive mode HCD tandem mass spectra showed the presence of the fragment ion characteristic of the PC head group at *m/z* 184, whereas the negative ion mode tandem mass spectra acquired at 5.1 and 6.1 min provided more detailed information on LPP structure. For example, the fragment ion at *m/z* 578.35 corresponded to the loss of formate and a methyl group, a characteristic loss for the PC head group. The most informative region was where anions of palmitic acid (*m/z* 255.23) and the five carbon long modified acyl chain with a C5 terminal aldehyde could be detected (*m/z* 155.04). The differences in MS/MS spectra taken at the different retention times can most likely be attributed to the *sn*-1/*sn*-2 positions of the two fatty acyl chains. Thus, the most intense signal eluting at 6.1 min most probably corresponds to 1-palmitoyl-2-(5-oxovaleroyl)-*sn*-glycero-3-phosphorylcholine whereas the signal at 5.6 min, which has a higher intensity of the *m/z* 115.04 ion, is probably due to the positional isomer 1-(5-oxovaleroyl)-2-palmitoyl-*sn*-glycero-3-phosphorylcholine [33,34]. Similarly, two chromatographic peaks were observed in the XIC at the mass of PGPC (**Supplementary Fig. S2**), and the XICs generated from both positive and negative mode data showed up to a three orders of magnitude increase in PGPC signal over the oxidation time course. The fragmentation data showed a different ratio between the anionic acyl chain fragment intensities (*m/z* 255.23 for palmitic and *m/z* 113.02 and 145.05 for glutaric acid), and the fragmentation spectra in negative ion mode were characterized by the diagnostic neutral loss of 59 Da from the parent (fragment at *m/z* 549.28), corresponding to loss of CH_3COOH from a terminal carboxylic acid, and the two fragment ions related to the short chain oxidized FA (*m/z* 113.02 and 145.05). These fragmentations with a Δm of 32 Da are due to the rearrangement of the polar head group, as has been described previously [35].

1-palmitoyl-2-(5-hydroxy-8-oxo-octenoyl)-*sn*-glycero-3-phosphorylcholine (HOOAPC), a previously reported short chain oxidized lipid in oxPAPC preparations, was also already present at time 0 h, and increased with time by up to two orders of magnitude (**Supplementary Fig. S3**). Once more, it was possible to identify the presence of two chromatographic peaks showing a different ratio between the intensities of the acyl chain anion signals. The loss of formate and methyl groups in negative ion mode and the polar head group PC characteristic fragments in positive ion mode were observed. A diagnostic ion confirming the hydroxyl group to be on an eight carbon long truncated acyl chain was present at *m/z* 153.06, resulting from water loss relative to the short chain oxidized FA (*m/z* 171.07).

Fig. 3 shows three examples of LC-MS/MS based identification of long chain oxPAPC species. In this case, the XICs are much more complex than for the short chain LPPs, indicating the presence of multiple isomeric species. For example, at least 11 different chromatographic peaks, 8 of them showing baseline separation, were detected for a mass corresponding to PAPC with the addition of one oxygen (**Fig. 3**). Furthermore, the chromatographic profile differed at the three oxidation time points. At 0 h all 11 peaks were present, while after 72 h some had disappeared. The fragmentation spectra in positive ion mode showed, as expected, a major fragment ion from the PC head group, but it was also possible to see a fragment ion resulting from the loss of 18 Da, corresponding to the loss of H_2O which is diagnostic of an OH group. Negative ion mode tandem mass spectra allowed the identification of many of the modification isomers. Thus, the isomeric PAPC oxidation products with a hydroxy (RT 13.1) or an epoxy (RT 13.9) group were identified based on the diagnostic ions at *m/z* 127.08 and 155.07 respectively, with the hydroxy group identified as being at position C7, and the epoxy group at C5-C6 (from the ion at *m/z* 191.18).

Supplementary Fig. S4 shows the identification of PAPC with the addition of two oxygens, where the XIC shows six main peaks at time points 0 h and 48 h, while at 72 h additional chromatographic peaks with shorter retention times were present. In positive ion mode the earlier eluting peaks showed one and two neutral losses of water molecules (-18 and -36 Da), typical of diHETE derivatives, while the later eluting signals were characterized by the neutral losses of 18 and 34 Da, diagnostic of lipid hydroperoxides. Furthermore, with these species for the first time we could identify in negative ion mode a diagnostic fragment ion (*m/z* 335.22) from the diHETE-PC, corresponding to arachidonic acid carrying two hydroxyl groups, whereas for the hydroperoxide containing oxPAPC the predominant signal was detected at *m/z* 317.21 (single water loss). Occasionally, it was even possible to detect a

signal at *m/z* 331.23 corresponding to [FA 20:4 + OOH - 2H] and characteristic fragments ions at 203.18 and 129.06 *m/z*, diagnostic for a hydroperoxide group at position C5.

Supplementary Fig. S5 demonstrates the identification of a long chain oxidized PAPC derivative characterized by the addition of three oxygen atoms and the loss of two hydrogens. The intensity over the oxidation time course increased by one order of magnitude between 0 and 48 h and then remained approximately constant. The most studied product with this mass is PEIPC. The fragmentation spectrum in negative ion mode is shown in **Supplementary Fig. 5B**. All previously reported [36] diagnostic fragment ions were present (*m/z* 331.19, 313.18, 305.21, 287.21, 269.19), including the characteristic ions for the epoxy group at the position C5-C6 (m/z 233.15, 215.14, 203.14, 147.07, 115.04). In positive ion mode the fragmentation spectra were characterized by the PC-specific fragment ion (184.07 *m/z*) and diagnostic OH neutral losses (loss of 18 and 36 Da).

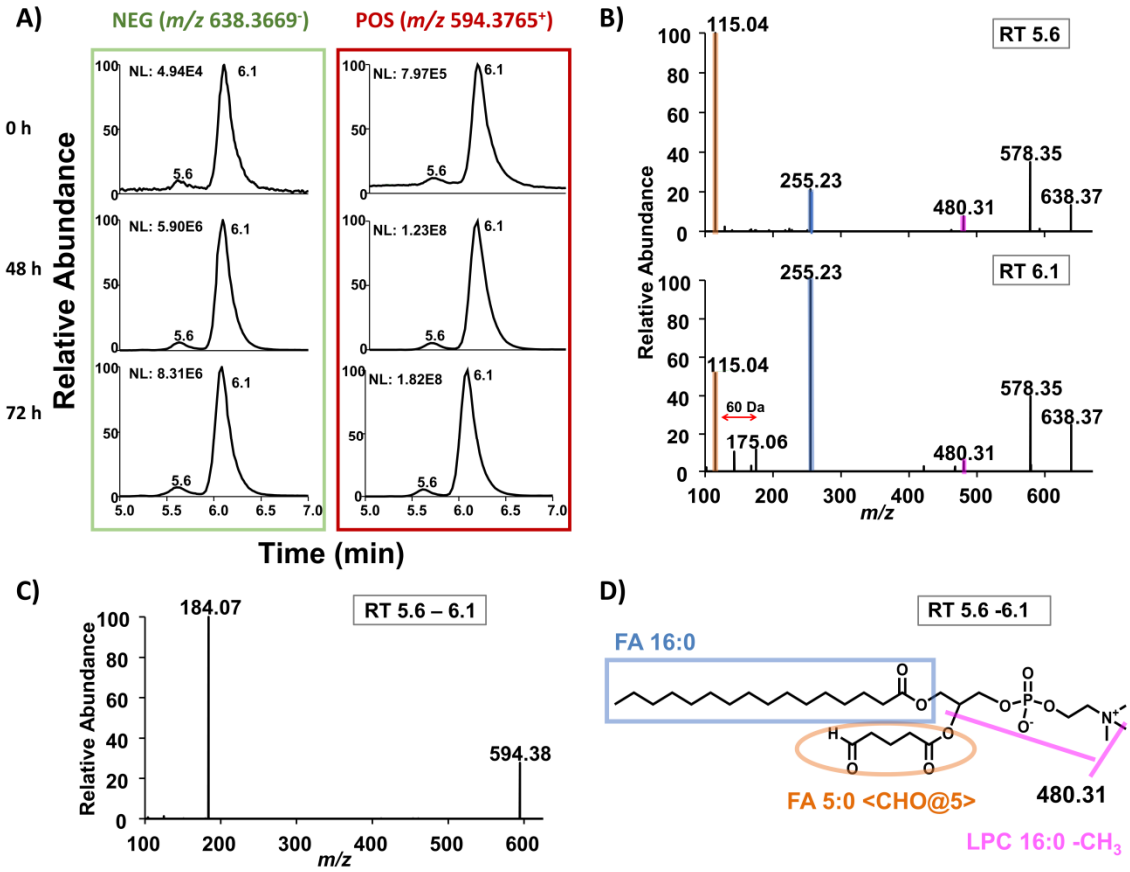

Fig. 2. Extracted ion chromatograms (A), HCD tandem mass spectra in negative (B), and positive ion modes (C) and proposed structure (D) of POVPC. Color-coding of structure-related signals in the negative mode MS/MS spectra (e.g. the anion of FA 16:0 in blue, oxFA in orange and green, and LPC fragment derived as NL of one FA in pink) corresponds to the color-coding of fragments assigned to proposed structures illustrated in the lower panel.

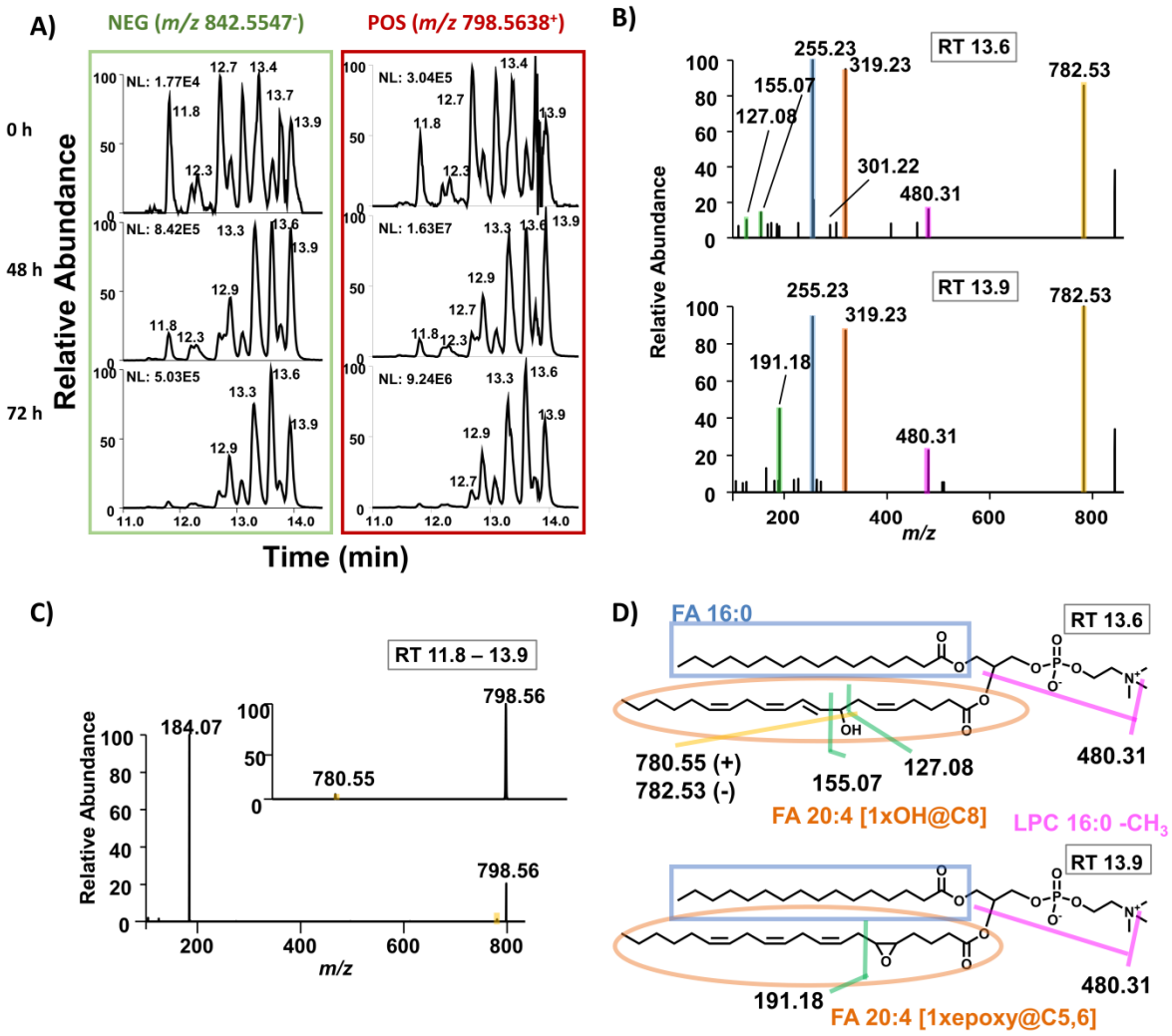

Fig. 3. Extracted ion chromatograms (A), HCD tandem mass spectra in negative (B), and positive ion mode (C) and proposed structure (D) of PAPC with the addition of one oxygen. Color-coding of structure-related signals in negative mode MS/MS spectra (e.g. the anion of FA 16:0 in blue, oxFA in orange and green, and LPC fragment derived as NL of one FA in pink) corresponds to the color-coding of fragments assigned to proposed structures illustrated in the lower panel.

3.3. Relative quantification of LPPs in air oxidized PAPC

15 LPPs, including lyso PCs (LPCs), short and long chain oxidation products, were selected for relative quantification (**Table 2**). Before evaluating the reproducibility of PAPC air oxidation in the four different laboratories, intra- and inter-laboratory analytical variability was examined.

Table 2. Elemental composition and proposed structures for the 15 LPPs in the oxPAPC mixture used for quantification. For each LPP the exact mass and *m/z* values for corresponding formate adduct (or *m/z* deprotonated ions in case of short chain LPPs with carboxylic acid terminal groups, marked with *) and protonated ions are provided.

Formula_ Neutral	Proposed structures	Exact mass	neg m/z $[M+HCOO^-]^-$	pos m/z $[M+H^+]^+$
$C_{24}H_{50}NO_7P$	LPC(16:0)	495.3325	540.3307	496.3398
$C_{28}H_{50}NO_7P$	LPC(20:4)	543.3325	588.3307	544.3398
$C_{29}H_{56}NO_9P$	PC(16:0/5:0<CHO@C5>)	593.3692	638.3669	594.3670
$C_{29}H_{56}NO_{10}P$	PC(16:0/5:0<COOH@C5>)	609.3636	608.3564*	610.3715
$C_{32}H_{60}NO_{10}P$	PC(16:0/8:1[1OH]<CHO@C8>)	649.3949	694.3931	650.4022
$C_{34}H_{62}NO_9P$	PC(16:0/10:2<CHO@C10>)	659.4157	704.4139	660.4235
$C_{37}H_{66}NO_9P$	PC(16:0/13:3<CHO@C13>)	699.4470	744.4452	700.4548
$C_{44}H_{78}NO_9P$	PC(16:0/20:4) +1O – 2H	795.5409	840.5391	796.5482
$C_{44}H_{80}NO_9P$	PC(16:0/20:4) +1O	797.5565	842.5547	798.5638
$C_{44}H_{76}NO_{10}P$	PC(16:0/20:4) +2O – 4H	809.5201	854.5183	810.5274
$C_{44}H_{80}NO_{10}P$	PC(16:0/20:4) +2O	813.5514	858.5496	814.5587
$C_{44}H_{78}NO_{11}P$	PC(16:0/20:4) +3O – 2H	827.5307	872.5289	828.5380
$C_{44}H_{80}NO_{11}P$	PC(16:0/20:4) +2O	829.5464	874.5446	830.5536
$C_{44}H_{80}NO_{12}P$	PC(16:0/20:4) +4O	845.5413	890.5395	846.5486
$C_{44}H_{78}NO_{13}P$	PC(16:0/20:4) +5O – 2H	859.5205	904.5187	860.5284

The LC-MS method used for relative LPP quantification had already been validated in different laboratories for the analysis of complex lipidomes [27,37]. To provide an estimation of the likely intra-lab accuracy of the quantification results for the LPPs, L4 evaluated intra-sample as well as analytical variation (CV%) by analyzing one experimental replicate of the oxPAPC preparation for each oxidation time point on three consecutive days. Normalized peak areas were calculated for both positive and negative ion modes (**Supplementary Table S2**). The coefficient of variation was under 20% for all LPPs at all time points, except for LPCs at time 0 h, which showed higher inter-day variability (up to 34%), probably as the storage of the oxPAPC sample over 3 days at -80 °C does not prevent the oxidation or hydrolysis process completely.

To assess inter-laboratory analytical variance, oxPAPC samples generated in L3 (0 and 72h oxidation) were analyzed in three different laboratories (L1, L3 and L4). Normalized peak areas were calculated and used to perform principle component analysis (PCA; **Supplementary Table S3**). As expected, the analyses for the 0 and 72 h time points are well separated on the PCA plot, whereas the analytical replicates are tightly clustered. The 0 h data is also well clustered, but there is clear separation at 72h for each laboratory. The first two principle components on the PCA scores plot (**Supplementary Fig. S6**) explain 85 % of the variation. The first principle component demonstrates separation based on the time of PAPC air exposure, whereas second principle component (explaining 18 % of the variation)

399 corresponds to separation based on inter-laboratory instrument variations; samples analysed
400 by L1 are grouped together at the bottom of the PCA scores plot, while L3 and L4 analysed
401 samples cluster more closely together. The minor variations explained by second principle
402 component (18%) are probably due to the type of mass analyzers used in the study (L1 - Q-
403 TOF mass spectrometer; L3 and L4 - quadrupole-Orbitrap MS).

404 Furthermore, to compare the impact of sample preparation at different locations with
405 the variation in analysis of a single, centrally prepared sample analyzed in different
406 laboratories, we performed PCA of the normalized peak areas of the 72h samples generated
407 in L3 and analysed in L1 (labeled L1a) and L4 (labeled L4a) and the samples generated
408 independently by the four laboratories and analysed in those laboratories (L1, L2, L3, and
409 L4) (**Supplementary Tables S3** and **S5**, **Fig. 4**). It is clear that the data for the sample
410 centrally generated in L3 but analysed at different locations cluster closely together and show
411 minimal variation, while the samples generated in different locations showed much higher
412 distribution. This demonstrates that the main variance was in the sample preparation, and that
413 the analysis of the same sample at different laboratories, using three different instruments
414 (L1:5600 TripleTOF, L3: Orbitrap Fusion™ Lumos™ Tribrid™ and L4: Q Exactive™
415 Plus), gave statistically very similar results. The reproducibility of analysis across the four
416 laboratories is supported by the 0 h data in **Supplementary Fig. S6**, which is also tightly
417 clustered.

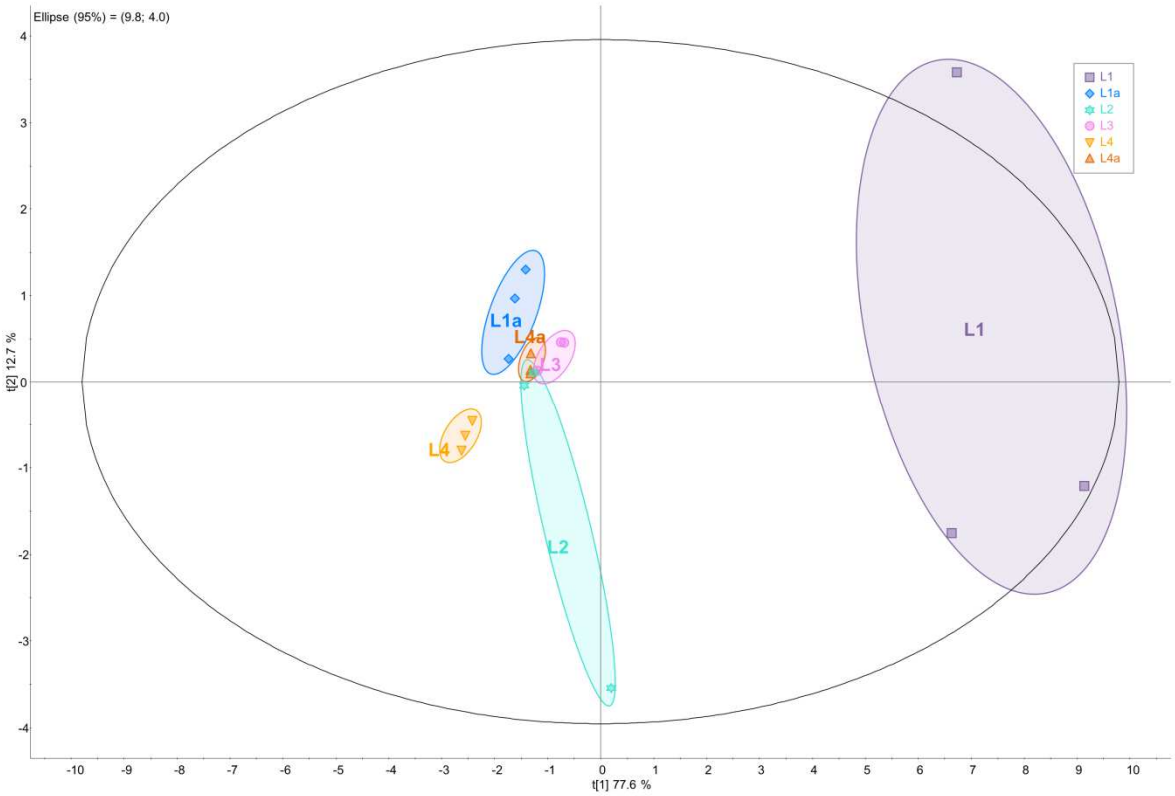

Fig. 4: PCA scores plot for normalized LPPs peak area in sample generated at 72h in L3 and analysed in three different laboratories (L1a, L3 and L4a), and samples prepared independently in the four laboratories (L1, L2, L3, L4). Violet squares – L1, blue squares – L1a, blue stars – L2, pink circles – L3, yellow triangle – L4, orange triangle – L4a.

Combining the results of the relative quantification of 15 LPPs from oxPAPC preparations produced and analyzed independently in four different laboratories (**Fig. 5**, **Table 3** and **Supplementary Table S4**), six LPPs were among the most abundant signals in all labs and could be routinely identified and quantified, and therefore were chosen to serve as representatives of the oxPAPC mixture at the 48 and 72 h time points.

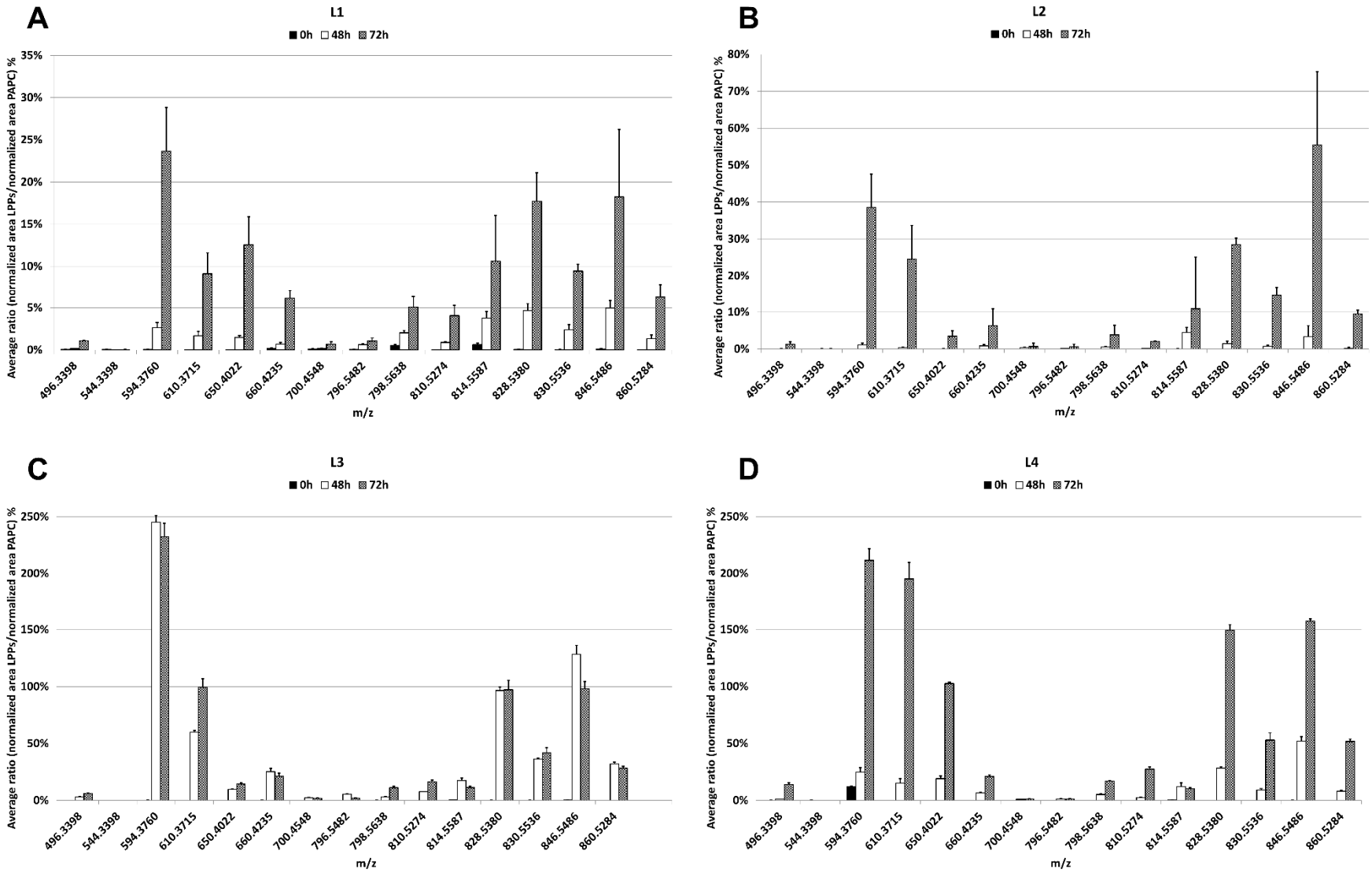

Fig. 5. Relative quantities (expressed as % of unmodified PAPC after the normalization to internal standard) of 15 representative LPPs from PAPC exposed to air oxidation for 0, 48 and 72 h. Graphs are shown for the time course at individual laboratories: L1 (A), L2 (B), L3 (C), and L4 (D) at 0 h, 48 h and 72 h. Identifications for each of the LPP masses can be found in S**upplementary Table S1**.

Table 3. The most abundant LPPs in air oxidized PAPC preparations for each laboratory (L1-L4) quantified relative to unmodified PAPC after normalization of corresponding peak areas to internal standard.

LPP, give as m/z values of protonated ions	**L1**	**L2**	**L3**	**L4**
594.38^{+}	24 %		232 %	211 %
610.37^{+}		39 %	99 %	195 %
650.40^{+}	13 %	25 %		103 %
814.56^{+}	11 %			
828.54^{+}	18 %	28 %	97 %	149 %
830.55^{+}		15 %	42 %	
846.55^{+}	18 %	55 %	98 %	157 %

These correspond to three short (*m/z* 594.38^{+}, 610.37^{+}, 650.40^{+}), and three long chain (m/z 828.55^{+}, 830.55^{+}, 846.55^{+}) LPPs. Based on the results of the MS/MS identifications, the short chain LPPs can be assigned to POVPC, PGPC and HOOAPC. For the long chain LPPs each *m/z* value, and thus elemental composition, can correspond to several isomeric species (**Table 2** and **Supplementary Table S1**). For instance, the LPP with elemental composition $C_{44}H_{78}NO_{11}P$ (*m/z* 828.55^{+}), usually referred to in oxPAPC mixtures as epoxyisoprostane E2 containing PC (PEIPC), could also be represented by the following combinations of the functional groups on a long chain LPP derived from AA: [OOH and keto], [2OH and keto], [2 epoxy and keto], and [epoxy, OH and keto]. The LPPs with elemental compositions $C_{44}H_{80}NO_{11}P$ (e.g. 3OH or OH + OOH) and $C_{44}H_{80}NO_{12}P$ (e.g. 4OH or 2OOH) are clearly represented by a mixture of isomeric structures, as some of these were at least partially separated by chromatography in this study. However, for the relative quantification reported here the total peak area for each *m/z* were combined to report overall abundance of all of the LPP isomers in order to be comparable with previously reported values for oxPAPC mixtures, which have commonly been analyzed by direct infusion methods where the isomeric species have not been differentiated.

Although the most abundant LPPs were essentially the same between all four participating laboratories, the abundances of oxidized lipids relative to unmodified PAPC were quite different (**Fig. 6**). Thus, after 48 h air exposure the oxPAPC prepared in L3 showed the highest oxidation levels, with POVPC being the most abundant LPP formed (245

% relative to unmodified PAPC). Among the long chain LPPs, the signals at *m/z* 846.55^{+} (128 %) and 830.54^{+} (96 %) were the highest after 48 h of air exposure. After 72 h exposure to the air oxidation, the highest LPPs quantities were detected in L4, with POVPC (211 %), PGPC (195 %) and long chain LPPs at *m/z* 846.55^{+} (149 %) and 830.54^{+} (157 %) being the most abundant.

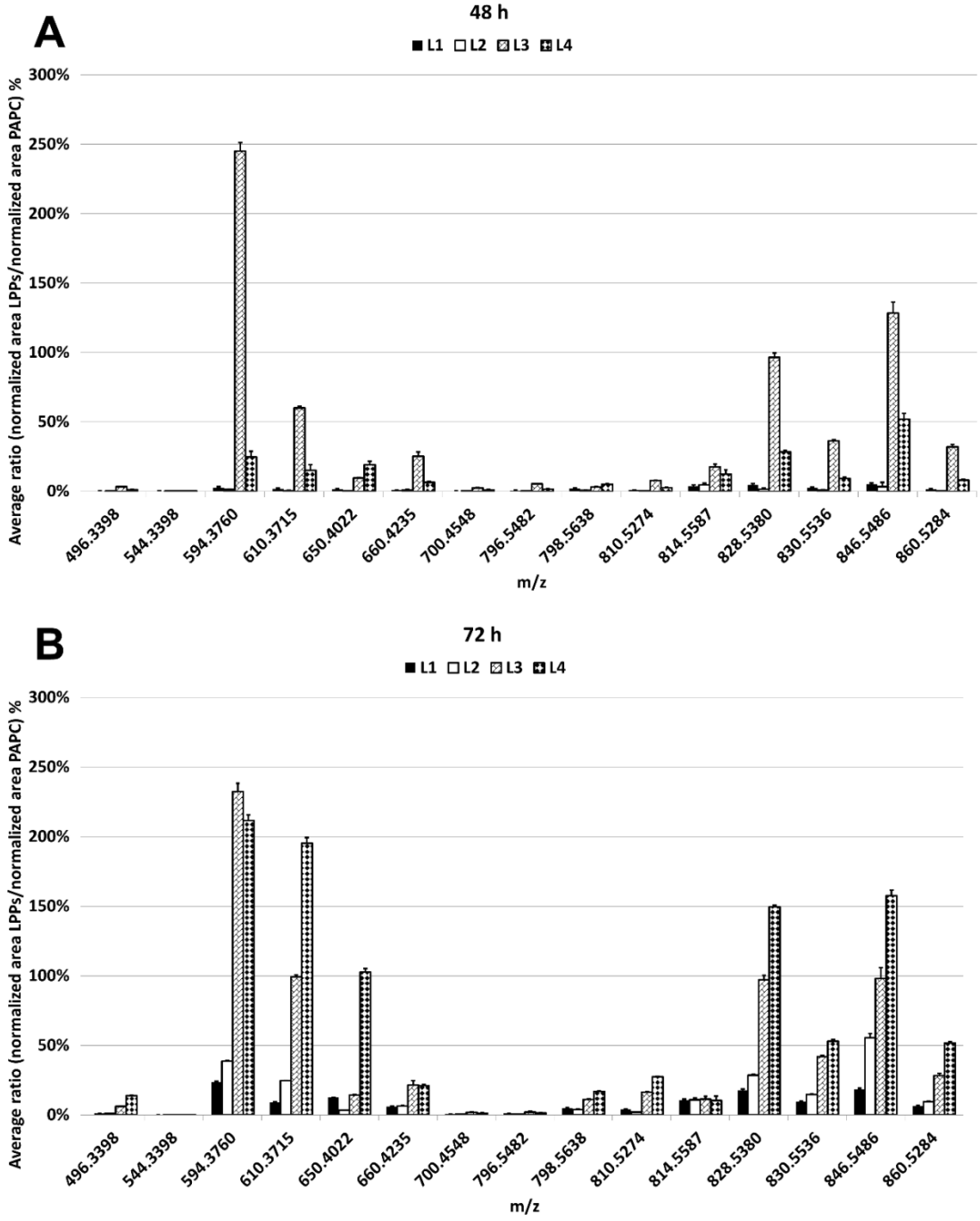

Fig. 6. Relative quantities (expressed as % of unmodified PAPC after the normalization to internal standard) of 15 LPPs in PAPC exposed to the air oxidation comparing directly the relative quantities identified in L1, L2, L3, and L4 at 48 (A) and 72 h (B).

Thus, overall relative abundances for the same LPPs produced in four laboratories differed markedly across the time course, and by up to 13.5-fold (e.g. signal at *m/z* 828.55^{+} in L1 and L4) even after 72 h of PAPC oxidation. The most variation between laboratories was seen at the 48 h time point and by 72 h the profiles in L2, 3 and 4 showed relatively similar overall abundance of oxidized products, although still with significant variation in individual species. In L1 the overall level of oxidation was still low even after 72 h. ANOVA analysis (**Table S5**) confirmed the statistical significance of the differences, with p-values below 0.05 for all quantified LPPs except PGPC at the 72 h time point.

One likely source of the difference in the oxidation rates could be small differences in the laboratory temperatures during PAPC air exposure, as average room temperatures in L1 were 22-25 °C, L2 16 °C, L3 28 °C, and L4 25 °C; this could result in changes in the rate of the initiation of the free radical oxidation, which is then amplified by the radical chain reaction. The laboratory temperature at which air oxidation of oxPAPC is performed is usually not reported in publications and might be a significant confounder in reported results. However, this is clearly not the only reason, as the L1 had the lowest level of oxidation throughout, but was not the coldest laboratory. Most importantly from the point of view of experiments that are dependent on bioactivity, there is clearly significant variability in the rate of reaction and the distribution of oxidized products produced.

Table 4. "Truncation score" (TS) for the oxPAPC preparations rom the four participating labs, calculated as the ratio between the summed abundances of three of the most abundant short chain LPPs (signal at *m/z* 594.38^{+}, 610.37^{+}, 650.40^{+}) to three of the most abundant long chain LPPs (signals at *m/z* 828.54^{+}, 830.55^{+}, 846.55^{+}).

	oxPAPC TS	
	48 h	**72 h**
L1	**0.48**	**1.00**
L2	**0.28**	**0.68**
L3	**1.21**	**1.46**
L4	**0.66**	**1.41**

In the literature, as a very general classification of bioactive compounds in air oxidized PAPC preparations, short chain LPPs are usually associated with pro-inflammatory effects whereas long chain LPPs are often associated with anti-inflammatory or protective functions

[17,24,25]. As is clear from the data presented above, despite the oxPAPC samples being generated in the four different laboratories using the same protocol, which required minimal sample manipulation (air exposure of the PAPC dried film), and each preparation giving rise to approximately the same set of abundant LPPs, there was a high variability in the total oxidation levels and in the extent of generation of individual LPPs. For this reason, a MS based evaluation for all in-house produced oxPAPC mixtures would be beneficial to clarify their exact composition before testing the biological effects.

Furthermore, a useful marker to help to characterize oxPAPC samples could be the ratio of short to long chain oxidation products, which we suggest could be called the "truncation score" (TS). This can be calculated for each oxPAPC preparation using the simple formula TS = ∑ % of short chain LPPs/∑ % of long chain LPPs. The TS calculated using, for example, the three most abundant species from each classification (**Table 3**), would be indicative of the ratio between short and long chain LPPs for each preparation, which is likely to be one of the most important characteristics for bioactivity. A TS value equal to one would indicate equal contribution of short and long chain LPPs, whereas TS > 1 and TS < 1 would correspond to the prevalence of short or long chain LPPs, respectively. The results from this study using the six most abundant species are shown in **Table 4**. This indicates that while the overall oxidation levels from L2 and L4 at 72 h look similar in the base peak chromatograms in **Fig. 1**, the preparation from L2 is higher in long chain components, while that for L4 is higher in short chain. Therefore, although TS is a very rough estimation for the prevalence of short over long chain LPPs, it could be used to evaluate the oxidation state balance of oxPAPC preparations before using them in biological experiments. It is not necessary to perform full LC-MS/MS characterization to determine the TS, as direct infusion MS data, which are usually obtained to validate PAPC oxidation by air exposure for in-house preparations, could be used.

One should also bear in mind that not it is not only the relative abundance of short chain over the long chain LPPs important, but their absolute concentrations are also highly significant. However, given the wide variety of chemical structures within oxPAPC mixture, and thus differences in ionization efficiency of LPPs with various functional groups, pure synthetic standards for each LPP class would be required to perform absolute quantification.

4. Conclusions

We have performed a multi-laboratory evaluation of air oxidized PAPC preparations from four different laboratories using LC-MS/MS analysis, focusing on the identification and

relative quantification of the LPPs formed. High intra-sample reproducibility and a very similar overall pattern of oxidation between the four laboratories was demonstrated. However, significant differences in the general extent of lipid oxidation relative to unmodified PAPC were observed. Thus, we propose that an MS based evaluation for all in house produced oxPAPC mixtures should be performed before using them to study biological effects of oxidized lipids. Furthermore, we suggest calculating the "truncation score" as a rough estimation of the balance between short vs long chain products of arachidonic acid oxidation.

Acknowledgments

Financial support from the EU H2020 funded project MASSTRPLAN (Grant number 675132; to all authors except TM) and German Federal Ministry of Education and Research (BMBF) within the framework of the e:Med research and funding concept for SysMedOS project (to MF) are gratefully acknowledged. Thanks are due to University of Aveiro, Marine Lipidomics Laboratory, Fundação para a Ciência e a Tecnologia (FCT, MECPortugal), European Union, QREN, Programa Operacional Factores de Competitividade (COMPETE) and FEDER for the financial support to QOPNA (FCT UID/QUI/00062/2019) and CESAM (UID/AMB/50017/2019) research units; Portuguese Mass Spectrometry Network (LISBOA-01-0145-FEDER-402-022125), FCT/MEC through national funds, and the co-funding by the FEDER, within the PT2020 Partnership Agreement and Compete 2020. We thank Prof. Ralf Hoffmann (Institute of Bioanalytical Chemistry, University of Leipzig) for providing access to his laboratory and Dr. Martin Zeller for scientific support and discussion.

Conflict of interests

The authors declare no conflict of interests.

Bibliography

[1] A. Trpkovic, I. Resanovic, J. Stanimirovic, D. Radak, S.A. Mousa, D. Cenic-Milosevic, D. Jevremovic, E.R. Isenovic, Oxidized low-density lipoprotein as a biomarker of cardiovascular diseases., Crit. Rev. Clin. Lab. Sci. 52 (2015) 70–85. doi:10.3109/10408363.2014.992063.

[2] D. Hasanally, A. Edel, R. Chaudhary, A. Ravandi, Identification of Oxidized

Phosphatidylinositols Present in OxLDL and Human Atherosclerotic Plaque., Lipids. 52 (2017) 11–26. doi:10.1007/s11745-016-4217-y.

[3] H. Itabe, K. Suzuki, Y. Tsukamoto, R. Komatsu, M. Ueda, M. Mori, Y. Higashi, T. Takano, Lysosomal accumulation of oxidized phosphatidylcholine-apolipoprotein B complex in macrophages: intracellular fate of oxidized low density lipoprotein., Biochim. Biophys. Acta. 1487 (2000) 233–245.

[4] V.N. Bochkov, Inflammatory profile of oxidized phospholipids., Thromb. Haemost. 97 (2007) 348–354.

[5] M. Aldrovandi, V.B. O'Donnell, Oxidized PLs and vascular inflammation., Curr. Atheroscler. Rep. 15 (2013) 323. doi:10.1007/s11883-013-0323-y.

[6] N. Leitinger, Oxidized phospholipids as triggers of inflammation in atherosclerosis., Mol. Nutr. Food Res. 49 (2005) 1063–1071. doi:10.1002/mnfr.200500086.

[7] N. Leitinger, The role of phospholipid oxidation products in inflammatory and autoimmune diseases: evidence from animal models and in humans., Subcell. Biochem. 49 (2008) 325–350. doi:10.1007/978-1-4020-8830-8_12.

[8] V.B. O'Donnell, M. Aldrovandi, R.C. Murphy, G. Kronke, Enzymatically oxidized phospholipids assume center stage as essential regulators of innate immunity and cell death., Sci. Signal. 12 (2019). doi:10.1126/scisignal.aau2293.

[9] J.A. Berliner, N. Leitinger, S. Tsimikas, The role of oxidized phospholipids in atherosclerosis., J. Lipid Res. 50 (2009) S207-12. doi:10.1194/jlr.R800074-JLR200.

[10] B. Burla, M. Arita, M. Arita, A.K. Bendt, A. Cazenave-Gassiot, E.A. Dennis, K. Ekroos, X. Han, K. Ikeda, G. Liebisch, M.K. Lin, T.P. Loh, P.J. Meikle, M. Orešič, O. Quehenberger, A. Shevchenko, F. Torta, M.J.O. Wakelam, C.E. Wheelock, M.R. Wenk, MS-based lipidomics of human blood plasma: a community-initiated position paper to develop accepted guidelines, J. Lipid Res. 59 (2018) 2001–2017. doi:10.1194/jlr.S087163.

[11] E.A. Dennis, P.C. Norris, Eicosanoid storm in infection and inflammation, Nat. Rev. Immunol. (2015) 511–523. doi:10.1038/nri3859.

[12] S. Yedgar, M. Krimsky, Y. Cohen, R.J. Flower, Treatment of inflammatory diseases by selective eicosanoid inhibition: a double-edged sword?, Trends Pharmacol. Sci. 28

(2007) 459–464. doi:10.1016/j.tips.2007.07.005.

[13] P. Bretscher, J. Egger, A. Shamshiev, M. Trotzmuller, H. Kofeler, E.M. Carreira, M. Kopf, S. Freigang, Phospholipid oxidation generates potent anti-inflammatory lipid mediators that mimic structurally related pro-resolving eicosanoids by activating Nrf2, EMBO Mol. Med. 7 (2015) 593–607. doi:10.15252/emmm.201404702.

[14] A.D. Watson, N. Leitinger, M. Navab, K.F. Faull, S. Hörkkö, J.L. Witztum, W. Palinski, D. Schwenke, R.G. Salomon, W. Sha, G. Subbanagounder, A.M. Fogelman, J.A. Berliner, Structural identification by mass spectrometry of oxidized phospholipids in minimally oxidized low density lipoprotein that induce monocyte/endothelial interactions and evidence for their presence in vivo, J. Biol. Chem. 272 (1997) 13597–13607. doi:10.1074/jbc.272.21.13597.

[15] N. Leitinger, T.R. Tyner, L. Oslund, C. Rizza, G. Subbanagounder, H. Lee, P.T. Shih, N. Mackman, G. Tigyi, M.C. Territo, J.A. Berliner, D.K. Vora, Structurally similar oxidized phospholipids differentially regulate endothelial binding of monocytes and neutrophils, Proc. Natl. Acad. Sci. 96 (1999) 12010–12015. doi:10.1073/pnas.96.21.12010.

[16] Y. Ke, N. Zebda, O. Oskolkova, T. Afonyushkin, E. Berdyshev, Y. Tian, F. Meng, N. Sarich, V.N. Bochkov, J.M. Wang, A.A. Birukova, K.G. Birukov, Anti-Inflammatory Effects of OxPAPC Involve Endothelial Cell-Mediated Generation of LXA4, Circ. Res. 121 (2017) 244–257. doi:10.1161/CIRCRESAHA.116.310308.

[17] A.A. Birukova, V. Starosta, X. Tian, K. Higginbotham, L. Koroniak, J.A. Berliner, K.G. Birukov, Fragmented oxidation products define barrier disruptive endothelial cell response to OxPAPC, Transl. Res. 161 (2013) 495–504. doi:10.1016/j.trsl.2012.12.008.

[18] N. Sarich, X. Tian, G. Gawlak, A.A. Birukova, K.G. Birukov, D.B. Sacks, Y. Tian, Role of IQGAP1 in endothelial barrier enhancement caused by OxPAPC, Am. J. Physiol. Cell. Mol. Physiol. 311 (2016) L800–L809. doi:10.1152/ajplung.00095.2016.

[19] C. Martin, C. Stoffer, M. Mohammadi, J. Hugo, E. Leipold, B. Oehler, H.L. Rittner, R. Blum, NaV1.9 Potentiates Oxidized Phospholipid-Induced TRP Responses Only under Inflammatory Conditions, Front. Mol. Neurosci. 11:7 (2018). doi:10.3389/fnmol.2018.00007.

[20] B. Oehler, K. Kistner, C. Martin, J. Schiller, R. Mayer, M. Mohammadi, R.S. Sauer, M.R. Filipovic, F.R. Nieto, J. Kloka, D. Pflücke, K. Hill, M. Schaefer, M. Malcangio, P.W. Reeh, A. Brack, R. Blum, H.L. Rittner, Inflammatory pain control by blocking oxidized phospholipid-mediated TRP channel activation, Sci. Rep. 7: 5447 (2017). doi:10.1038/s41598-017-05348-3.

[21] I. Zanoni, Y. Tan, M. Di Gioia, J.R. Springstead, J.C. Kagan, By Capturing Inflammatory Lipids Released from Dying Cells, the Receptor CD14 Induces Inflammasome-Dependent Phagocyte Hyperactivation, Immunity. 47 (2017) 697–709. doi:10.1016/j.immuni.2017.09.010.

[22] I. Zanoni, Y. Tan, M. Di Gioia, A. Broggi, J. Ruan, J. Shi, C.A. Donado, F. Shao, H. Wu, J.R. Springstead, J.C. Kagan, An endogenous caspase-11 ligand elicits interleukin-1 release from living dendritic cells, Science (80-.). 352 (2016) 1232–1236. doi:10.1126/science.aaf3036.

[23] L.H. Chu, M. Indramohan, R.A. Ratsimandresey, A. Gangopadhyay, E.P. Morris, D.M. Monack, A. Dorfleutner, C. Stehlik, The oxidized phospholipid oxPAPC protects from septic shock by targeting the non-canonical inflammasome in macrophages, Nat. Commun. 9:996 (2018). doi:10.1038/s41467-018-03409-3.

[24] P. Karki, K.G. Birukov, Lipid mediators in the regulation of endothelial barriers., Tissue Barriers. 6 (2018) e1385573. doi:10.1080/21688370.2017.1385573.

[25] V. Bochkov, B. Gesslbauer, C. Mauerhofer, M. Philippova, P. Erne, O. V. Oskolkova, Pleiotropic effects of oxidized phospholipids, Free Radic. Biol. Med. 111 (2017) 6–24. doi:10.1016/j.freeradbiomed.2016.12.034.

[26] C. Mauerhofer, M. Philippova, O. V Oskolkova, V.N. Bochkov, Hormetic and anti-inflammatory properties of oxidized phospholipids., Mol. Aspects Med. 49 (2016) 78–90. doi:10.1016/j.mam.2016.02.003.

[27] A. Criscuolo, M. Zeller, K. Cook, G. Angelidou, M. Fedorova, Rational selection of reverse phase columns for high throughput LC-MS lipidomics., Chem. Phys. Lipids. 221 (2019) 120–127. doi:10.1016/j.chemphyslip.2019.03.006.

[28] Z. Ni, G. Angelidou, R. Hoffmann, M. Fedorova, LPPtiger software for lipidome-specific prediction and identification of oxidized phospholipids from LC-MS datasets,

649 Sci. Rep. 7: 15138 (2017). doi:10.1038/s41598-017-15363-z.

650 [29] B. Davis, G. Koster, L.J. Douet, M. Scigelova, G. Woffendin, J.M. Ward, A. Smith, J.
651 Humphries, K.G. Burnand, C.H. Macphee, A.D. Postle, Electrospray ionization mass
652 spectrometry identifies substrates and products of lipoprotein-associated phospholipase
653 A2 in oxidized human low density lipoprotein, J. Biol. Chem. 283 (2008) 6428–6437.
654 doi:10.1074/jbc.M709970200.

655 [30] E.A. Podrez, E. Poliakov, Z. Shen, R. Zhang, Y. Deng, M. Sun, P.J. Finton, L. Shan,
656 M. Febbraio, D.P. Hajjar, R.L. Silverstein, H.F. Hoff, R.G. Salomon, S.L. Hazen, A
657 novel family of atherogenic oxidized phospholipids promotes macrophage foam cell
658 formation via the scavenger receptor CD36 and is enriched in atherosclerotic lesions, J.
659 Biol. Chem. 277 (2002) 38517–38523. doi:10.1074/jbc.M205924200.

660 [31] E. Fahy, S. Subramaniam, R.C. Murphy, M. Nishijima, C.R.H. Raetz, T. Shimizu, F.
661 Spener, G. van Meer, M.J.O. Wakelam, E.A. Dennis, Update of the LIPID MAPS
662 comprehensive classification system for lipids, J. Lipid Res. 50 (2009) S9–S14.
663 doi:10.1194/jlr.R800095-JLR200.

664 [32] M. Lange, Z. Ni, A. Criscuolo, M. Fedorova, Liquid Chromatography Techniques in
665 Lipidomics Research, Chromatographia. 82 (2019) 77–100. doi:10.1007/s10337-018-
666 3656-4.

667 [33] H. Nakanishi, Y. Iida, T. Shimizu, R. Taguchi, Separation and quantification of sn-1
668 and sn-2 fatty acid positional isomers in phosphatidylcholine by RPLC-ESIMS/MS, J.
669 Biochem. 147 (2010) 245–256. doi:10.1093/jb/mvp171.

670 [34] K. Wozny, W.D. Lehmann, M. Wozny, B.S. Akbulut, B. Brügger, A method for the
671 quantitative determination of glycerophospholipid regioisomers by UPLC-ESI-
672 MS/MS, Anal. Bioanal. Chem. 411 (2019) 915–924. doi:10.1007/s00216-018-1517-5.

673 [35] A.C. Almstrand, C. Johnson, R.C. Murphy, Evidence for an N-methyl transfer reaction
674 in phosphatidylcholines with a terminal aldehyde during negative electrospray
675 ionization tandem mass spectrometry, Anal. Bioanal. Chem. 407 (2015) 5045–52.
676 doi:10.1007/s00216-015-8555-z.

677 [36] G. Subbanagounder, J.W. Wong, H. Lee, K.F. Faull, E. Miller, J.L. Witztum, J.A.
678 Berliner, Epoxyisoprostane and epoxycyclopentenone phospholipids regulate

679 monocyte chemotactic protein-1 and interleukin-8 synthesis. Formation of these
680 oxidized phospholipids in response to interleukin-1β, J. Biol. Chem. 277 (2002) 7271–
681 81. doi:10.1074/jbc.M107602200.

682 [37] E. Rampler, A. Criscuolo, M. Zeller, Y. El Abiead, H. Schoeny, G. Hermann, E.
683 Sokol, K. Cook, D.A. Peake, B. Delanghe, G. Koellensperger, A novel lipidomics
684 workflow for improved human plasma identification and quantification using RPLC-
685 MSn methods and isotope dilution strategies, Anal. Chem. 90 (2017) 6494–6501.
686 doi:10.1021/acs.analchem.7b05382.

687 [38] V.N. Bochkov, O. V. Oskolkova, K.G. Birukov, A.-L. Levonen, C.J. Binder, J. Stöckl,
688 Generation and Biological Activities of Oxidized Phospholipids, Antioxid. Redox
689 Signal. 12 (2009) 1009–1059. doi:10.1089/ars.2009.2597.

690

Highlights

- Multi-laboratory evaluation of air oxidized PAPC preparations by LC-MS/MS.
- Identification and relative quantification of lipid peroxidation products (LPPs).
- oxPAPC preparations should be characterized by MS prior testing biological effects of oxidized lipids.
- “Truncation score” is proposed as a rough estimation of oxPAPC oxidation status.